

Article

Investigation of Mechanical Properties, Durability and Microstructure of Low-Clinker High-Performance Concretes Incorporating Ground Granulated Blast Furnace Slag, Siliceous Fly Ash and Silica Fume

Katarzyna Konieczna * , Karol Chilmon and Wioletta Jackiewicz-Rek * 

Faculty of Civil Engineering, Warsaw University of Technology, Al. Armii Ludowej 16, 00-637 Warsaw, Poland; k.chilmon@il.pw.edu.pl

* Correspondence: k.konieczna@il.pw.edu.pl (K.K.); wjr@il.pw.edu.pl (W.J.-R.)

Abstract: The main assumption of eco-efficient High-Performance Concrete (HPC) design is the reduction of Portland cement clinker content without negatively affecting the composite's mechanical and durability properties. In this paper, three low-clinker HPC mixtures incorporating slag cement (CEM III/B as per EN 197-1) and Supplementary Cementitious Materials (SCMs)—Ground Granulated Blast Furnace Slag (GGBFS), Siliceous Fly Ash (SFA) and Silica Fume (SF)—were designed. The maximum amount of Portland cement clinker from CEM III/B varied from 64 to 116 kg in 1 m³ of concrete mix. The compressive strength of HPC at 2, 7, 14, 28, 56, 90 days, and 2 years after casting, as well as the modulus of elasticity on 2-year-old specimens, was tested. The depth of water penetration under pressure and internal frost resistance in freeze–thaw tests were evaluated after 56 days of curing. Additionally, the concrete pH value tests were performed. The microstructure of 2-year-old HPC specimens was analyzed using Scanning Electron Microscopy (SEM). The research proved that it is possible to obtain low-clinker High-Performance Concretes that reach compressive strength of 76–92 MPa after 28 days of curing, show high values of modulus of elasticity (49–52 GPa) as well as increased resistance to frost and water penetration under pressure.

Keywords: high-performance concrete; low-clinker cement; ground granulated blast furnace slag



Citation: Konieczna, K.; Chilmon, K.; Jackiewicz-Rek, W. Investigation of Mechanical Properties, Durability and Microstructure of Low-Clinker High-Performance Concretes Incorporating Ground Granulated Blast Furnace Slag, Siliceous Fly Ash and Silica Fume. *Appl. Sci.* **2021**, *11*, 830. <https://doi.org/10.3390/app11020830>

Received: 5 December 2020

Accepted: 10 January 2021

Published: 17 January 2021

Publisher's Note: MDPI stays neutral with regard to jurisdictional claims in published maps and institutional affiliations.



Copyright: © 2021 by the authors. Licensee MDPI, Basel, Switzerland. This article is an open access article distributed under the terms and conditions of the Creative Commons Attribution (CC BY) license (<https://creativecommons.org/licenses/by/4.0/>).

1. Introduction

According to the PBL Netherlands Environmental Assessment Agency report [1], Portland cement clinker production is one of the key drivers of global CO₂ emissions. Production of Ordinary Portland Cement (OPC), which consists of more than 95% Portland cement clinker, exceeded a level of 4 billion metric tons in 2019 and is expected to increase by 25% over in the next 10 years [2,3]. Since the production of 1 ton of OPC generates nearly 900 kg of CO₂ [4], the global trend is to reduce the amount of OPC in concrete mixes by using binary cements, as well as partially replacing it with supplementary cementitious materials (SCMs) such as Ground Granulated Blast Furnace Slag (GGBFS), Siliceous Fly Ash (SFA) and Silica Fume (SF) [5–7]. Slag cement CEM III/B (as per EN 197-1) is characterized by an embodied CO₂ value of 232–359 kg CO₂e/t, which is more than two times lower than OPC. For GGBFS and fly ash, these values are significantly lower: 79.6 kg CO₂e/t and 0.1 kg CO₂e/t, respectively [4]. The environmental impact of OPC production is an issue that cannot be ignored, especially in the design process of High-Performance Concretes (HPC), which are not only characterized by high compressive strength (from 50–60 MPa to 100–120 MPa at 28 days) as a result of low water/binder ratio, but also by the high modulus of elasticity, high density and enhanced durability in comparison to normal strength concretes [8].

Based on the literature review, it can be stated that the above-mentioned criteria can be met using binary cements with a high GGBFS amount (e.g., CEM III/B). Thanks to

the latent hydraulic properties of GGBFS, its activation in the presence of cement clinker occurs at an appropriate concentration of Ca^{2+} , OH^- , SO_4^{2-} ions and alkali in the solution. As reported by Pal et al. [9], GGBFS C-S-H hydrates add density to the cement paste, as they are more gel-like than the OPC hydration products. The incorporation of GGBFS in normal, high-strength and ultra-high-strength concretes results in the improvement in the pore structure and durability properties of the composite, such as increased electrical resistivity and reduced chloride penetration, as stated by many researchers [10–14]. As reported by Shi [15] and Zhang [16], in HPC design, particular attention should be paid to the qualitative and quantitative selection of SCMs due to the high sensitivity of durability to changes in mineral additives content and water/binder ratio. The use of GGBFS in low emission HPCs can also be potentially beneficial in terms of an effective reduction of the water/binder ratio. As reported in the review article of Matthes et al. [5], CEM III/B with 72% content of GGBFS presented higher sensitivity to polycarboxylate-based superplasticizer dosage than OPC. These observations encouraged researchers to design low-clinker and high-GGBFS HPCs with the use of highly effective superplasticizers. However, the effectiveness of GGBFS to reduce superplasticizer demand is considered to decrease with an increase of GGBFS fineness and/or at low water/binder ratios (<0.30) [5].

As reported by Teng et al. [12], the use of Ultra-Fine GGBFS (UFGGBFS) improves the mechanical and durability properties of High Strength Concretes (HSC). The researchers observed that the 30% replacement of OPC with UFGGBFS made it possible to increase the HSC compressive strength at a very early age and achieve a higher modulus of elasticity after 28 days of curing compared to mixes with 100% OPC. Moreover, the effectiveness of UFGGBFS was greater for mixtures with a lower water/cementitious materials ratio. However, HPCs with a low water/binder ratio are especially prone to cracking due to the autogenous shrinkage under restrained conditions. This could be prevented by incorporating fibers into the cement matrix, i.e., polymer or steel fibers. The use of fibers significantly enhances the tensile strength and ductility of the cement-based materials and hence improves their durability [17].

According to the research conducted by Giergiczny et al. [18], low CO_2 emission High-Performance Concretes reaching a compressive strength of 100 MPa after 90 days of curing can be successfully designed using multicomponent Portland and slag cements. The non-air-entrained HPCs with a clinker content of 211–269 kg per 1 m^3 of concrete and addition of silica fume were considered to be frost-resistant after 28 days of curing with an average compressive strength loss not greater than 3.5% after 150 cycles of freezing and thawing (according to Polish procedure PN-B-06265). High resistance to water penetration under pressure was also observed for these low-clinker High-Performance Concretes. In the paper of Atis and Bilim [19], high-strength concretes with a water/binder ratio equal to 0.30 and 20–40% replacement of OPC with GGBFS were characterized by a compressive strength above 80 MPa after 28 days of curing, exceeding the values obtained for a reference concrete mixture with 100% OPC as a binder. Lämmlein et al. [20] stated that it was possible to obtain low-clinker self-compacting HPCs with OPC content of 134–204 kg in 1 m^3 of concrete mix by incorporating fly ash, limestone, silica fume, and metakaolin. The designed HPCs reached compressive strength ranging from 77 to 88 MPa after 28 days of curing. Research into the synergistic effect of GGBFS, FA and SF addition on the microstructure, as well as mechanical and durability properties, has already been conducted for normal strength concretes by Dave et al. [21].

Based on the literature search, it can be stated that in the vast majority of studies, the properties of low-clinker concretes are evaluated for up to 90 days. The amount of research concerning longer periods of curing is limited. Therefore, further investigation needs to be done in this field, especially in the case of low-clinker HPC.

In this paper, the properties of High-Performance Concretes with low Portland cement clinker content were investigated. Slag cement (CEM III/B) was used as the main binder in the designed concrete mixtures. SCMs such as Ground Granulated Blast Furnace Slag (GGBFS), Siliceous Fly Ash (SFA) and Silica Fume (SF) were added in various proportions,

maintaining a low water/binder ratio (0.30) in order to achieve high compressive strength in the composite. The concretes' long-term mechanical performance was investigated on the basis of compressive strength and modulus of elasticity tests conducted 2 years after specimen preparation. Additionally, SEM microstructure analysis was performed on 2-year-old samples. Durability properties were assessed on the basis of freeze–thaw tests and water penetration under pressure tests, along with a hardened concrete pH value testing after 56 days of curing.

2. Materials and Methods

2.1. Materials

Slag cement CEM III/B 42.5 L–LH/SR/NA containing from 66 to 80% of ground granulated blast furnace slag (GGBFS) was used as a main binder in the HPC mix design. Additionally, SCMs such as Ground Granulated Blast Furnace Slag (GGBFS), Siliceous Fly Ash (SFA), and Silica Fume (SF) were used in ternary and quaternary binder systems. The physical and mechanical properties of cement are shown in Table 1. Table 2 presents the specific surface area and chemical composition of cement and supplementary cementitious materials.

Table 1. Physical and mechanical properties of CEM III/B 42.5 L–LH/SR/NA.

Water Demand (%)	Setting Time (min)		Compressive Strength (MPa)			Flexural Strength (MPa)		
	Initial Setting	Final Setting	7 d	28 d	56 d	7 d	28 d	56 d
32.5	247	317	27.8	54.3	60.7	6.2	10.6	10.6

Table 2. Specific surface area and chemical composition of cementitious materials.

Material	Specific Surface Area	Chemical Composition (%)						
		CaO	SiO ₂	Al ₂ O ₃	Fe ₂ O ₃	MgO	SO ₃	K ₂ O
C	0.5315 m ² /g *	50.60	32.87	6.85	1.61	3.53	2.29	0.49
GGBFS	0.9102 m ² /g **	46.08	37.58	6.96	0.54	6.11	1.54	0.50
FA	0.8504 m ² /g **	-	47.61	23.21	15.26	-	-	4.57
SF	22.9113 m ² /g **	0.18	97.86	-	0.38	0.24	-	0.84

* Blaine method, ** BET method, (-) range undetectable by means of the analysis.

Hydraulic reactivity of GGBFS was assessed by means of hydraulic modulus (CaO + MgO)/SiO₂ and the total amount of CaO + MgO + SiO₂ calculations as proposed in EN 15167-1. As the hydraulic modulus of the used GGBFS was equal to 1.39 and the total amount of CaO + MgO + SiO₂ was greater than 67%, it can be stated that the material met the European standard requirements for use in concrete and was characterized by a satisfactory reactivity.

HPC grading curve (Figure 1) was designed to match DIN 1045-2 standard requirements using river sand 0/2 mm (specific gravity of 2.63) (FA 0–2) and two fractions of coarse basalt aggregates, 2–8 mm (CA 2–8) and 8–16 mm (CA 8–16), with specific gravities of 3.05 and 3.04, respectively.

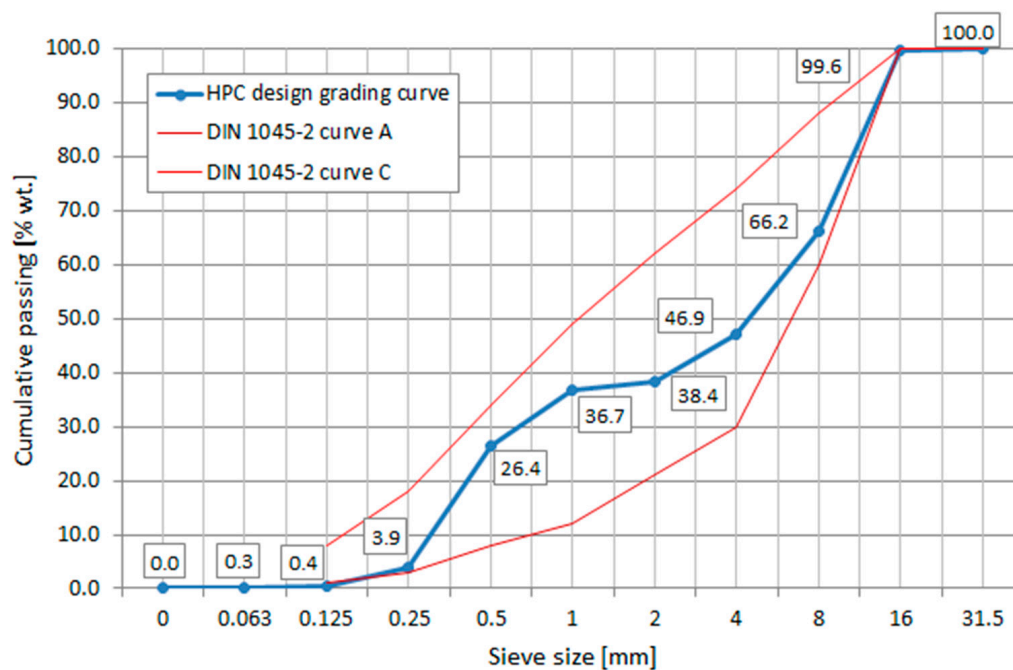


Figure 1. HPC grading curve with target DIN 1045-2 grading.

The main goal of the grading curve design process was to obtain minimum void content and the maximum packing density of the aggregate skeleton. To obtain a satisfactory degree of workability and maintain the low water/binder ratio of the concrete mix, highly effective polycarboxylate ether-based superplasticizers (SP) were used. No air-entraining admixtures were added.

2.2. Mixture Proportions and Specimen Preparation

Three High-Performance Concrete mixtures with a limited Portland cement clinker content were designed, as reported in Table 3.

Table 3. HPC mix compositions.

Mixture	Ingredient Content [kg/m ³]									w/b Ratio ¹	Max. Portland Cement Clinker Content [kg/m ³]
	C	GGBFS	SFA	SF	Water	FA 0–2	CA 2–8	CA 8–16	SP		
C55_SFA15_SF3	187	153	51	10.2	121	790	561	728	4.2	0.30	64
C100_SFA15_SF3	340	-	51	10.2	121	774	550	713	4.2		116
C100_SFA30_SF3	340	-	102	10.2	136	739	525	680	4.2		116

¹ w/b ratio = $m_{\text{water}} / (m_{\text{C}} + \text{GGBFS} + \text{FA} + \text{SF})$.

For C100_SFA15_SF3 and C100_SFA30_SF3 mixtures, ternary binder systems were applied (i.e., cement (C), fly ash (FA) in an amount of 15% or 30% cement mass and silica fume (SF) in an amount of 3% cement mass). In the case of the C55_SFA15_SF3 mixture, a quaternary binder system was designed by additionally replacing 45% of the cement (C) with GGBFS. Therefore, assuming 34% to be the maximum content of Portland cement clinker in the mass of CEM III/B 42,5 L–LH/SR/NA main components (as per EN 197-1), the maximum content of Portland cement clinker in the designed HPC mixes was estimated to be at levels of 26 wt% and 29 wt% of total cementitious materials for C100_FA15_SF and C100_SFA30_SF3, respectively. The maximum Portland cement clinker content in C55_SFA15_SF3 mixtures was stated to be equal to 16 wt% of total cementitious materials. The water/binder ratio was defined as a ratio of the mass of water to the total mass of cement and SCMs. Similar workability of all mixes was assumed, with a slump value range

of 100–150 mm according to the PN-EN 12350-2 standard requirements of the S3 slump consistency class.

Cylindrical ($d = 150$ mm, $h = 300$ mm) and cubic ($100 \times 100 \times 100$ mm and $150 \times 150 \times 150$ mm) specimens were prepared for testing the mechanical and durability properties of HPC according to EN 12390-2. All samples except the cylindrical specimens for the modulus of elasticity tests were cured in water at (20 ± 1) °C until the tests. Specimens for the modulus of elasticity tests were cured under the above-mentioned conditions for 90 days and then moved to the laboratory room (temperature = (22 ± 2) °C, relative humidity = 30–50%), where they were stored until testing.

2.3. Testing Methods

The consistency of fresh concrete mixes was evaluated by conducting slump tests in accordance with EN 12350-2.

The compressive strength of HPC was tested on $100 \times 100 \times 100$ mm specimens after 2, 7, 14, 28, 56, and 90 days of curing following the EN 12390-3 standard. Compression tests were conducted on the three-sample series using a CONTROLS MC66 press. Specimens smaller than the standard $150 \times 150 \times 150$ mm size were used due to the expected high concrete strengths and, consequently, high values of maximum force to be applied to samples.

The modulus of elasticity was determined in compression tests on 2-year-old cylindrical specimens ($d = 150$ mm, $h = 280$ mm) according to the procedure described in EN 12390—13 Method A. Cylindrical specimens with a height of 300 mm were trimmed to 280 mm in order to obtain 2-cm-thick slice specimens for SEM/EDS testing. The compressed surface of samples was prepared by grinding. Three electronic compressometers (Figure 2) with a gauge length of 150 mm and $0.02 \mu\text{m}$ sensitivity were used to measure longitudinal strains. Each test consisted of two preloading checks (wiring stability and specimen positioning check) and three loading cycles with a maximum loading equal to one-third of the estimated mix design compressive strength. The modulus of elasticity was calculated as the stabilized secant modulus of elasticity. Tests were performed on CONTROLS MC66 press on two-sample series. To estimate compressive strength, two cylindrical samples of each mix design were tested according to the EN 12390-3 procedure.



Figure 2. Modulus of elasticity testing.

Freeze–thaw resistance tests were carried out following the procedure presented in the Polish standard PN-B-06265 after 56 days of curing. Two six-sample series of the 100 mm concrete cubes were subjected to cyclic freezing and thawing. After saturation in the water at $(+18 \pm 2) ^\circ\text{C}$ for 7 days, the first series of specimens was weighed, and then subjected to 150 cycles of freezing at $(-18 \pm 2) ^\circ\text{C}$ for 4 h and thawing at $(+18 \pm 2) ^\circ\text{C}$ for 2–4 h. The second series of six specimens was stored in water at a temperature of $(+18 \pm 2) ^\circ\text{C}$ during the entire period of freeze–thaw resistance testing. After the last freeze–thaw cycle, the specimens from series 1 were again weighed, and their compressive strength was tested and compared to the compressive strength of the reference specimens. The test results were average mass loss and average percentage reduction in sample compressive strength after freezing and thawing. Concrete is regarded as being resistant to frost if the average mass loss is less or equal to 5% and the reduction of compressive strength is no greater than 20%.

Depth of water penetration under pressure tests were conducted on two 150 mm cube samples after 56 days of curing according to EN 12390-8. After the application of water pressure to the specimen surface, the penetration depth was measured. A maximum water penetration depth of 30 mm was set as the limit value.

The Scanning Electron Microscope (SEM) with Electron Dispersion Spectroscopy (EDS) method was used to evaluate the concrete microstructure and phase composition. FEI Nova NanoSEM 200 microscope equipped with EDAX Octane Elect EDS was used. The observations were made in a low vacuum mode (80 Pa), operating at 15 kV voltage using a vCD detector. Cross-sectional slice samples obtained from the upper 2 cm of the cylindrical specimens for the modulus of elasticity tests were used in the analysis. Before the SEM/EDS tests, the samples' surfaces were prepared by polishing using Struers Tegramin automatic polisher, and the samples were dried.

The pH values of hardened concrete were measured after 56 days of curing on two samples for each mix design. After grinding the specimens in a crusher, 1:1 solutions of finely crushed concrete combined with distilled water were prepared (Figure 3) and subjected to pH value tests in the Metrohm 781 pH/Ion Meter device after 24 h of conditioning under laboratory conditions.

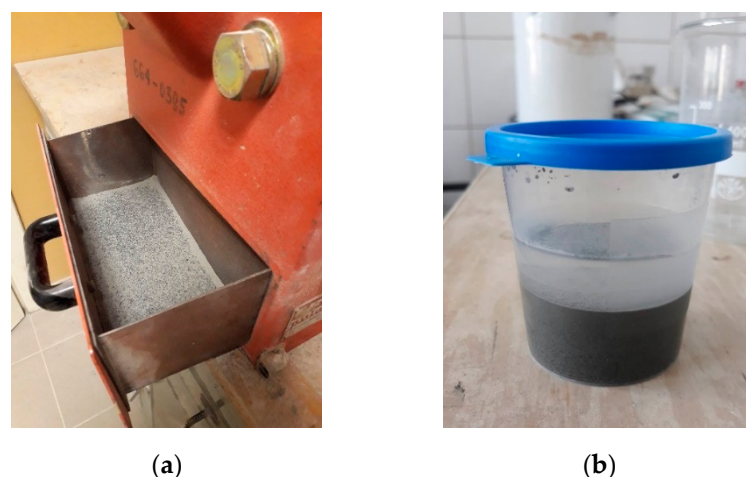


Figure 3. Concrete pH testing procedure: (a) specimen after grinding; (b) finely crushed concrete: distilled water 1:1 solution.

The chemical composition of cement and SCMs was determined by the X-Ray Fluorescence (XRF) method using a Bruker S4 EXPLORER spectrometer.

The specific surface area of cement was measured by the Blaine method according to the EN 196-6 procedure and, in the case of GGBFS, SFA and SF, using the BET method from the nitrogen adsorption at 78 K using ASAP 2020 Micromeritics apparatus.

3. Results and Discussion

3.1. Consistency of Fresh Concrete

All low-clinker HPC mixtures met the requirements of the S3 slump class, with slump values equal to 150 mm for C55_SFA15_SF3 mixture, 130 mm for C100_SFA15_SF3 mixture and 120 mm for C100_SFA30_SF3 mixture. It can be stated that the use of highly effective superplasticizers made it possible to obtain satisfactory workability of the mixtures while maintaining a low water/binder ratio. However, fresh concrete mixtures were characterized by high cohesiveness, which is considered typical for concretes containing a low amount of water and major amounts of GGBFS as well as silica fume addition [22]. Comparing slump test results obtained for mixtures C55_SFA15_SF3 and C100_SFA15_SF3, it can be stated that a partial replacement of cement with GGBFS had a positive effect on the workability of the concrete mixture. One of the causes of this phenomenon could be the lower specific surface area and glassy surface texture of GGBFS particles, which results in lower water demand for the cementitious binder blend. In the case of the C100_SFA30_SF3 mixture with an increased share of siliceous fly ash, no significant deterioration of the concrete mixture workability was observed compared to the C100_SFA15_SF3 mixture.

3.2. Compressive Strength

Figure 4 presents average compressive strength values of HPC after 2, 7, 14, 28, 56 and 90 days of curing (tested on 100 mm cube specimens), as well as 2 years (730 days) after specimen preparation (tested on 150 mm/300 mm cylinders). To unify the analysis process, the tested compressive strength values were converted into those corresponding to 150 mm cubic specimens using conversion factors for HPC: 0.99 and 0.86 for 100 mm cubic and cylindrical specimens, respectively [23].

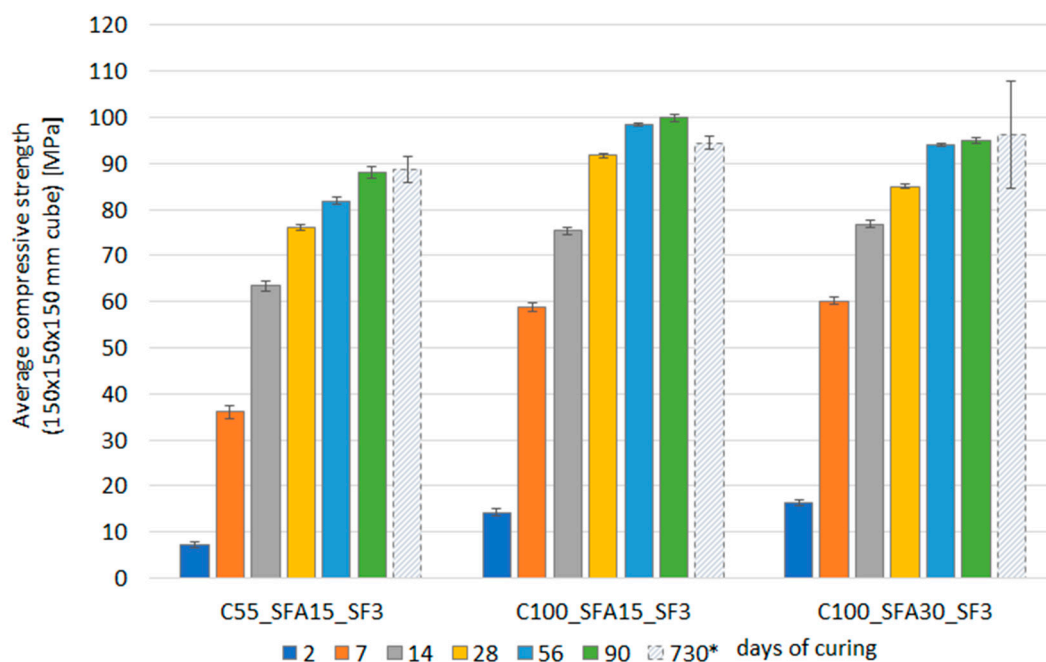


Figure 4. Average compressive strength of low-clinker HPC; *—compressive strength values tested on two specimens, converted using conversion factor of 0.86 for cylindrical specimens.

Due to the possible lower accuracy of the cylinder-cube strength value conversion and dispersion of the results obtained on cylindrical specimens, it can be concluded that the compressive strength of low-clinker HPC mixtures increased continuously over time. Additionally, it can be stated that within the period of 90 days to 730 days after specimen preparation, a less significant increase in concrete strength was observed (0.8–1.4%) than within the 28–90 days curing period (9–16%). This could be caused by a change in the

storage conditions of cylindrical specimens. Comparing compressive strength values of C100_SFA15_SF3 mixture and a corresponding mixture C55_SFA15_SF3 with a 45% replacement of cement by GGBFS, it can be seen that the compressive strength of HPC decreased with an increase of GGBFS content. The biggest differences between these two mixtures were found in the case of early strength, with 50% and 39% lower strength values at 2 and 7 days of curing being obtained for the C55_SFA15_SF3 mixture. After 28 days of curing, the compressive strength of the designed low-clinker HPC varied between 76.1 and 91.7 MPa. It should be highlighted that for the C100_SFA30_SF3 mixture, the increase in the FA content in comparison to C100_SFA15_SF3 mixture did not lead to an increase in the compressive strength.

All concretes were characterized by relatively low early strength (7.2–16.3 MPa after 2 days of curing). According to the EN 206 standard, the rate of compressive strength development of the designed HPC at 20 °C was assessed by calculating the ratio of the average compressive strength after 2 days of curing ($f_{cm,2}$) to the average compressive strength after 28 days of curing ($f_{cm,28}$). The calculation results are presented in Table 4.

Table 4. Rate of compressive strength development for HPC mixtures according to EN 206.

Mixture	$f_{cm,2}/f_{cm,28}$ Ratio	Compressive Strength Development Rate at 20 °C
C55_SFA15_SF3	0.09	very slow
C100_SFA15_SF3	0.16	slow
C100_SFA30_SF3	0.19	slow

Based on the calculations, the rate of compressive strength development for HPC mixtures containing 100% CEM III/B as the main binder was described as slow, whereas the C55_SFA15_SF3 mixture with a reduced amount of Portland cement clinker was characterized by a very slow increase in compressive strength. The evaluation of the long-term compressive strength development rate was done by comparing the values of compressive strength on the 28th and 90th days of concrete curing. The following values of the $f_{cm,28}/f_{cm,90}$ ratio were obtained: 0.87 for the C55_SFA15_SF3 mixture, 0.89 for the C100_SFA15_SF3 mixture and 0.92 for the C100_SFA30_SF3 mixture. It can be stated that the compressive strength development rates were similar, unlike in the case of the $f_{cm,2}/f_{cm,28}$ ratio. The average increase in the compressive strength between the 28th and 90th days of curing was equal to 12%, while the highest value of 16% was obtained for the C55_SFA15_SF3 mixture.

The obtained compressive strength values have been compared with time-dependent concrete strength development models proposed in:

- ACI Committee 209 [24]:

$$f_c(t) = \beta_{cc}(t) \cdot f_{c28}, \quad (1)$$

$$\beta_{cc}(t) = \frac{t}{a + b \cdot t} \quad (2)$$

- JSCE [25]:

$$f_c(t) = d \cdot \beta_{cc}(t) \cdot f_{c28}, \quad (3)$$

$$\beta_{cc}(t) = \frac{t}{a + b \cdot t} \quad (4)$$

- and Eurocode 2 (EN 1992-1-1), MC 2010 [26,27]:

$$f_c(t) = \beta_{cc}(t) \cdot f_{c28}, \quad (5)$$

$$\beta_{cc}(t) = e^{s[1 - \{\frac{28}{t}\}^{0.5}]} \quad (6)$$

where $f_c(t)$ is the compressive strength of concrete at an age of t days in MPa, f_{c28} is the compressive strength of concrete at an age of 28 days, and d, β_{cc} are coefficients, the values of which depend on cement type and strength class.

As the above-mentioned models were created to predict compressive strength development of concretes containing mainly OPC, the strength development of the designed HPC was predicted using coefficients suggested by Klemczak et al. [28] and Mierzwa [29] for concretes containing GGBFS, as reported in Table 5. A comparison of the test results with the models is presented in Figure 5 and Table 6.

Table 5. Coefficients applied in time-dependent compressive strength development models.

Model	Coefficients
ACI Committee 209	$a = 4.0, b = 0.85$ [28]
JSCE	$d = 1.15, a = 6.2, b = 0.93$ [28]
Eurocode 2 (EN 1992-1-1), MC 2010	$s = 0.20$ [29]

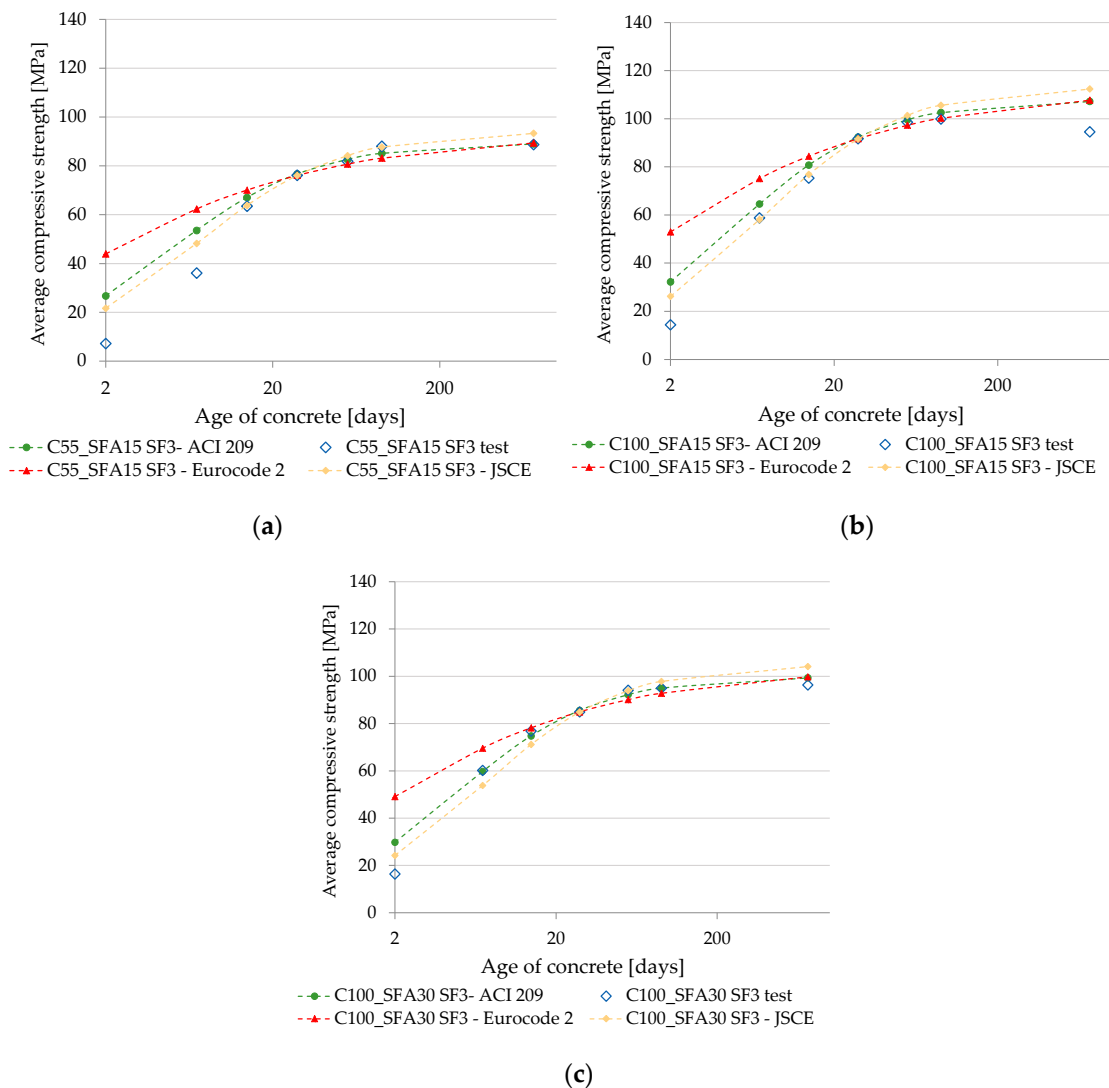


Figure 5. Comparison of compressive strength test results with time-dependent strength development models: (a) C55_SFA15_SF3 mix; (b) C100_SFA15_SF3 mix; (c) C100_SFA30_SF3 mix.

Table 6. Differences between tested and model-predicted compressive strength values.

Mixture	Model	Tested Value/Predicted Value Difference [%]						
		2	7	14	28 *	56	90	730
C55_SFA15_SF3	ACI Committee 209	+271.0	+48.2	+5.6	-	+0.9	−3.3	+0.3
	JSCE	+201.7	+33.4	+0.4	-	+2.8	−0.4	+5.1
	Eurocode 2,MC 2010	+511.1	+72.5	+10.4	-	−1.4	−5.5	+0.8
C100_SFA15_SF3	ACI Committee 209	+124.7	+9.8	+7.2	-	+1.1	+2.7	+13.4
	JSCE	+82.7	−1.2	+2.0	-	+2.9	+5.7	+18.9
	Eurocode 2,MC 2010	+270.1	+27.8	+12.0	-	−1.3	+0.3	+14.0
C100_SFA30_SF3	ACI Committee 209	+82.5	−0.7	−2.6	-	−2.0	0.0	+3.1
	JSCE	+48.4	−10.6	−7.4	-	−0.2	+3.0	+8.1
	Eurocode 2,MC 2010	+200.5	+15.5	+1.8	-	−4.3	−2.3	+3.6

*—the actual value of the 28-day compressive strength was used for model calculations.

Analyzing the results obtained in an early curing period, it can be stated that the predicted 2-day compressive strength values were vastly greater than the experimental values for each of the time-dependent models. The most significant overestimation of early compressive strength was observed for the Eurocode 2 and MC 2010 standards. Significant differences between early strength test results and values predicted using this model were also observed for High-Strength Concretes with slag cement CEM III/A 32.5 N in the article of Mierzwa [29]. Starting from the 7th day of curing for the C100_SFA15_SF3 and C100_SFA30_SF3 mixtures and the 14th day for the C55_SFA15_SF3 mixture, a gradual decrease in the difference between the tested and calculated values was observed. This observation confirms the conclusion presented in Table 4 regarding the slow and very slow compressive strength development of HPCs with a low Portland cement clinker content. Based on the predicted strength values after 28 days of curing, it can be confirmed that HPC containing slag and mineral additives can achieve compressive strength comparable to concretes with OPC in the long curing period. However, the commonly used time-dependent strength development models do not describe the rate of low-clinker HPC strength gain sufficiently, especially in an early curing period.

3.3. Modulus of Elasticity

The results of the modulus of elasticity tests are shown in Figure 6. The mean values obtained on 730-day-old specimens ranged from 48.64 GPa (C55_SFA15_SF3) to 51.80 GPa (C100_SFA30_SF3). A correlation between compressive strength and elastic modulus values was observed: the HPC with the lowest mean compressive strength (C55_SFA15_SF3) was also the one with the lowest mean elastic modulus. For the mixtures with higher compressive strengths (C100_SFA30_SF3 and C100_SFA15_SF3), the mean values of elastic modulus were approximately 6% higher than those obtained for C55_SFA15_SF3.

The obtained results were compared (Table 7) with the values estimated by the three different models recommended for HSC by ACI 363 [30], Eurocode 2 (EN 1992-1-1) [26] and NS 3473 [31] standards, respectively:

$$E_c = 3.32\sqrt{f_c} + 6.9 \quad (7)$$

$$E_c = 22(0.1 \cdot f_c)^{\frac{1}{3}} \quad (8)$$

$$E_c = 9.5(f_c)^{\frac{1}{3}} \quad (9)$$

where f_c is the cylinder mean compressive strength in MPa, and E_c is the modulus of elasticity in GPa.

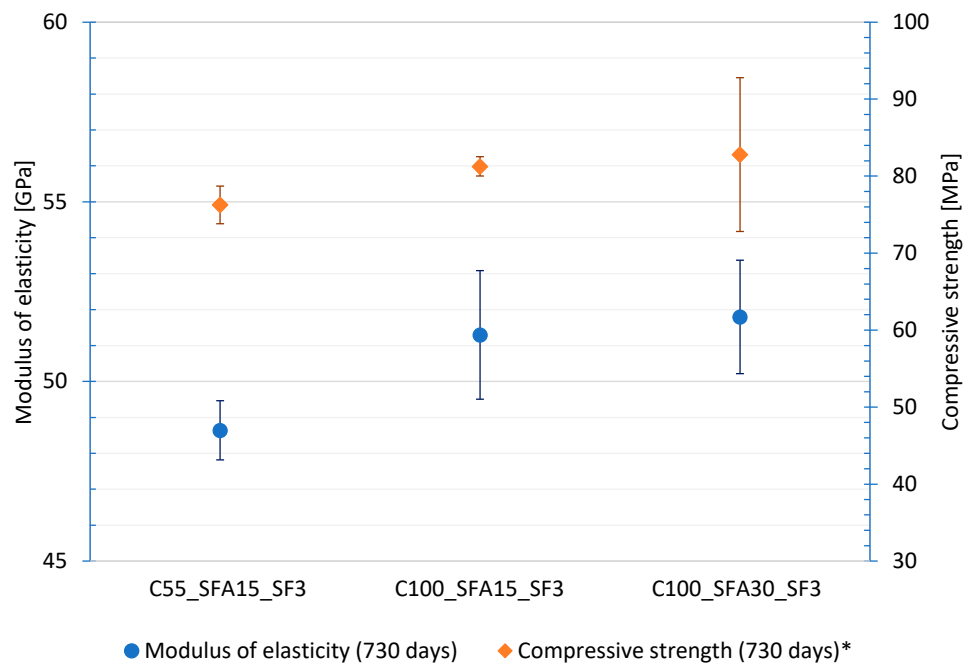


Figure 6. Average modulus of elasticity and compressive strength values for HPC (730 days after specimen preparation); *—compressive strength values obtained on cylindrical specimens.

Table 7. Comparison between modulus of elasticity values obtained from tests (according to EN 12390-13) and those estimated by three different models: ACI 363 [30], EN 1992-1-1 [26] and NS 3473 [31].

Mixture	Modulus of Elasticity [GPa]			
	Tested Value (Mean)	Estimated Value		
		ACI 363	Eurocode 2	NS 3473
C55_SFA15_SF3	48.64	35.89	43.30	40.29
C100_SFA15_SF3	51.29	36.83	44.23	41.15
C100_SFA30_SF3	51.79	37.11	44.51	41.41

The significant differences observed between obtained and estimated values could be explained by the use of coarse basalt aggregate and the fact that modulus of elasticity was tested on 730-day-old samples. The Eurocode 2 (EN 1992-1-1) [26] indicates that the modulus of elasticity estimated from Equation (8) should be increased by 20% when basalt coarse aggregate is used in concrete. In such cases, the recalculated estimated values would be 51.90 GPa (C55_SFA15_SF3), 53.04 GPa (C100_SFA15_SF3) and 53.41 GPa (C100_SFA30_SF3).

In the same standard [26], it has been pointed out that the concrete age has a significant influence on its modulus of elasticity. Thus, the secant modulus of elasticity of concrete at the age of t days should be estimated from the following equation:

$$E_{cm}(t) = (f_c(t)/f_c)^{0.3} \cdot E_{cm} \tag{10}$$

where $E_{cm}(t)$ is the modulus of elasticity at the age of t days in GPa, $f_c(t)$ is the cylinder compressive strength of concrete at the age of t days in MPa, f_c is the compressive strength of concrete at the age of 28 days, and E_{cm} is the modulus of elasticity at the age of 28 days in GPa estimated from Equation (8).

Given Equation (10), the estimated modulus of elasticity values of concrete at the age of 730 days would be equal to 52.41 GPa (C55_SFA15_SF3), 57.36 GPa (C100_SFA15_SF3) and 54.18 GPa (C100_SFA30_SF3).

It could be concluded that none of the recommended models allows the estimation of the modulus of elasticity of tested concretes with acceptable precision. Estimated values were 26–28% lower (ACI 363) or 17–20% lower (NS 3473) than the tested values. In the case of EN 1992-1-1, the values estimated from Equation (8) were 11–14% lower than those tested, but given the correction regarding used coarse aggregate and age of concrete, the recalculated values were 5–12% higher than those tested, leading to the conclusion that the C100_SFA15_SF3 mixture could be characterized by a modulus of elasticity equal to 57.37 GPa, which is highly unlikely to be obtained for concrete composites.

3.4. Frost Resistance

The results of the HPC internal frost resistance after 56 days of curing are presented in Table 8. It can be stated that all the designed non-air-entrained concretes met the requirements of maximum average mass loss (5%) and the maximum reduction of compressive strength (20%) after 150 cycles of freezing and thawing. No cracks were found on the surfaces of the samples. The C55_SFA15_SF3 concrete with quaternary binder mix combination showed the best performance with the lowest value of mass loss and fully maintained compressive strength after testing. The reason for the high observed internal frost resistance in the designed low-clinker HPC was considered to be the formation of a dense binder (cement-GGBFS-FA-SF) matrix with low porosity and high homogeneity.

Table 8. Internal frost resistance of low-clinker HPC.

Mixture	Avg. Specimen Mass [kg]		Average Mass Loss [%]	Avg. Compressive Strength [MPa]		Avg. Compressive Strength Retained [%]
	Before F-T Test	After F-T Test		Reference	F-T treated	
C55_SFA15_SF3	2.491	2.488	0.12	81.45	81.15	100
C100_SFA15_SF3	2.498	2.494	0.19	98.60	93.93	95
C100_SFA30_SF3	2.494	2.490	0.16	93.04	89.16	96

3.5. Depth of Water Penetration under Pressure

For the two HPC mixtures with the lowest internal frost resistance, as described in Section 3.3, the depth of water penetration under pressure was determined on two specimens. Based on the results presented in Table 9, it can be concluded that the designed HPCs were characterized by high resistance to water penetration under pressure and met the requirement for penetration depth not exceeding 30 mm after 56 days of curing. The HPC mixture with 30% fly ash content (C100_SFA30_SF3) showed slightly greater resistance to water penetration than C100_SFA15_SF3 concrete, which is consistent with the results obtained in the frost resistance tests and indicates the important role of SCMs (FA) in creating a dense concrete structure. No leakage was observed in any of the samples.

Table 9. Depth of penetration of water under pressure for HPC with 100% CEM III/B as a main binder.

Mixture	Depth of Penetration of Water under Pressure [mm]
C100_SFA15_SF3	10 15
C100_SFA30_SF3	12 10

3.6. Scanning Electron Microscopy (SEM) with EDS Analysis

Backscattered Electron (BSE) SEM images presenting the microstructure of samples from each mixture are shown in Figure 7. Phase compositions of cement matrices were confirmed by means of the EDS analysis, the results of which are shown in Figure 8.

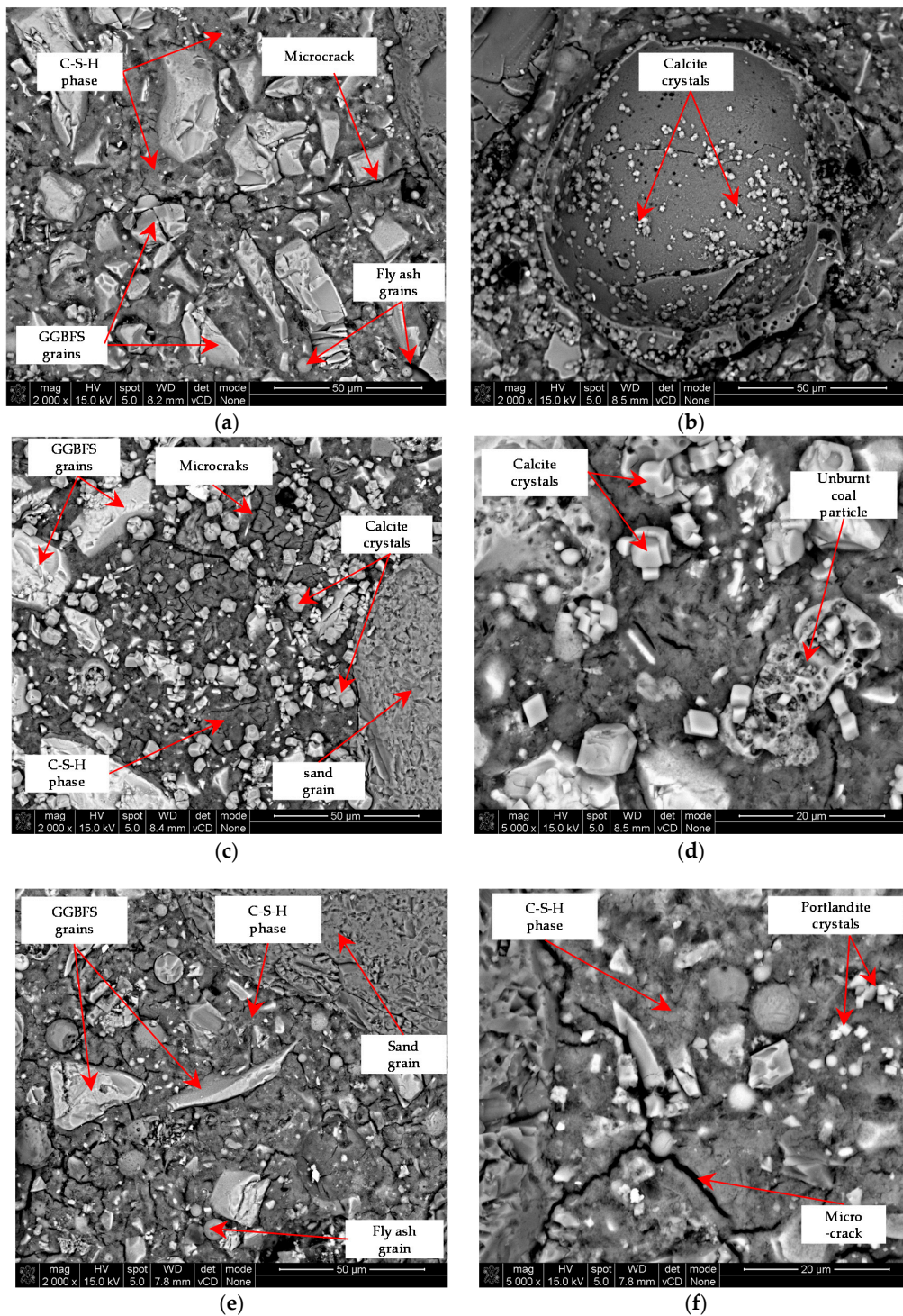
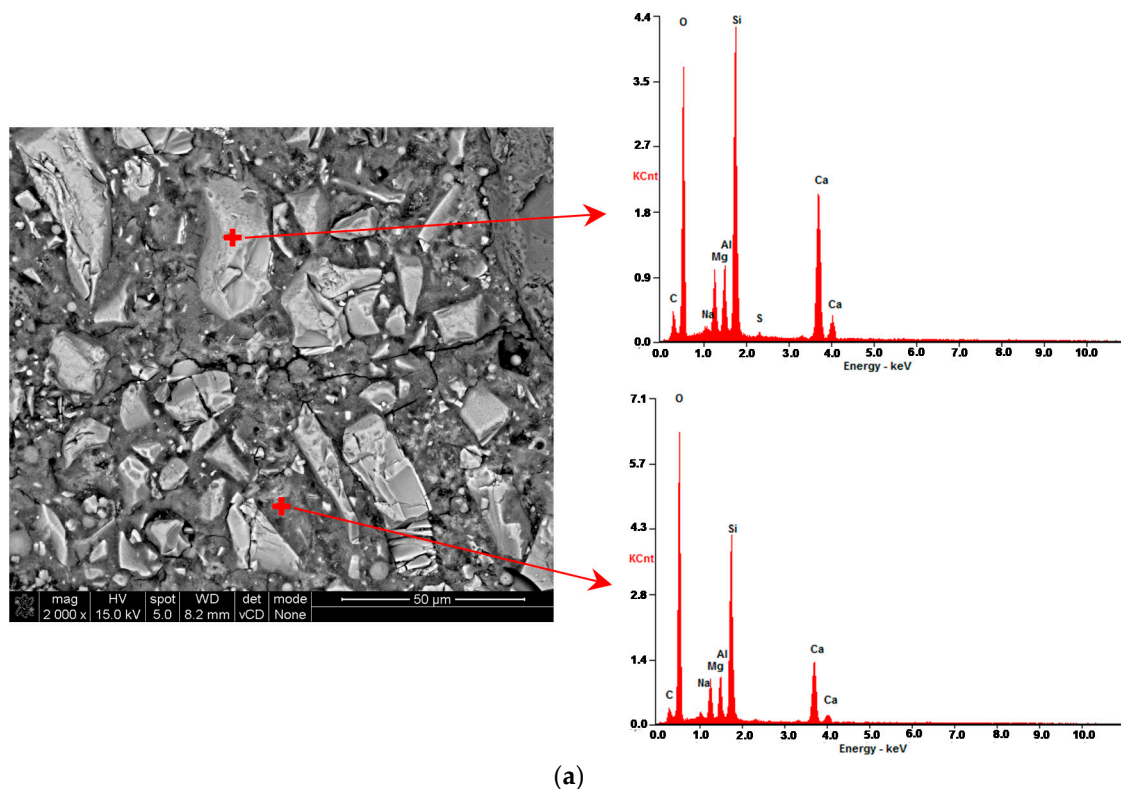


Figure 7. SEM images (BSE) presenting the microstructures of the (a,b) C55_SFA15_SF3, (c,d) C100_SFA15_SF3, and (e,f) C100_SFA30_SF3 samples.

The cement matrix structure in all samples was dense and consisted mainly of the C-S-H phase and unhydrated GGBFS grains (Figure 7a–f). The highest number of unhydrated

GGBFS grains was observed in the C55_SFA15_SF3 sample, as it contained the highest amount of GGBFS. Some unreacted fly ash grains (Figure 7a,c,e) and unburnt coal particles (Figure 7d) were also visible, but in much lower quantities. Characteristic cubic crystals of calcite (Figure 7d), as an effect of portlandite carbonation, were present inside pores and in the cement matrix of all samples, but in different amounts. The sample with the lowest amount of GGBFS and SFA (C100_SFA15_SF3) contained significantly more calcite crystals at the same depth compared with other mixes. This could be explained by previous studies indicating that the reduction of the amount of Portland cement clinker is associated with the reduction of the amount of portlandite ($\text{Ca}(\text{OH})_2$) in concrete [32]. Some Portlandite crystals (Figure 7f) were identified in all samples, but the amounts were not significant.

Microcracks in the cement matrix were present in all mixes, though with a different intensity. The sample with the lowest amount of Portland cement clinker (C55_SFA15_SF3) contained a significantly lower number of microcracks than the other mixes. The high amount of microcracks might be associated with the fact that the SEM samples were obtained from the near-to-surface layer of concrete, which is especially prone to shrinkage-induced microcracking. However, due to the sample preparation method and the lack of shrinkage measurements, it is impossible to clearly determine whether the observed differences were associated with the higher amount of Portland cement clinker. Microcracks in the cement-based composites have easily been induced by the sample cutting and drying prior to SEM observations [33]. The cutting process generates a direct mechanical impact on the sample, while during drying, a moisture gradient is developed, causing tensile stresses associated with drying shrinkage.



(a)
Figure 8. Cont.

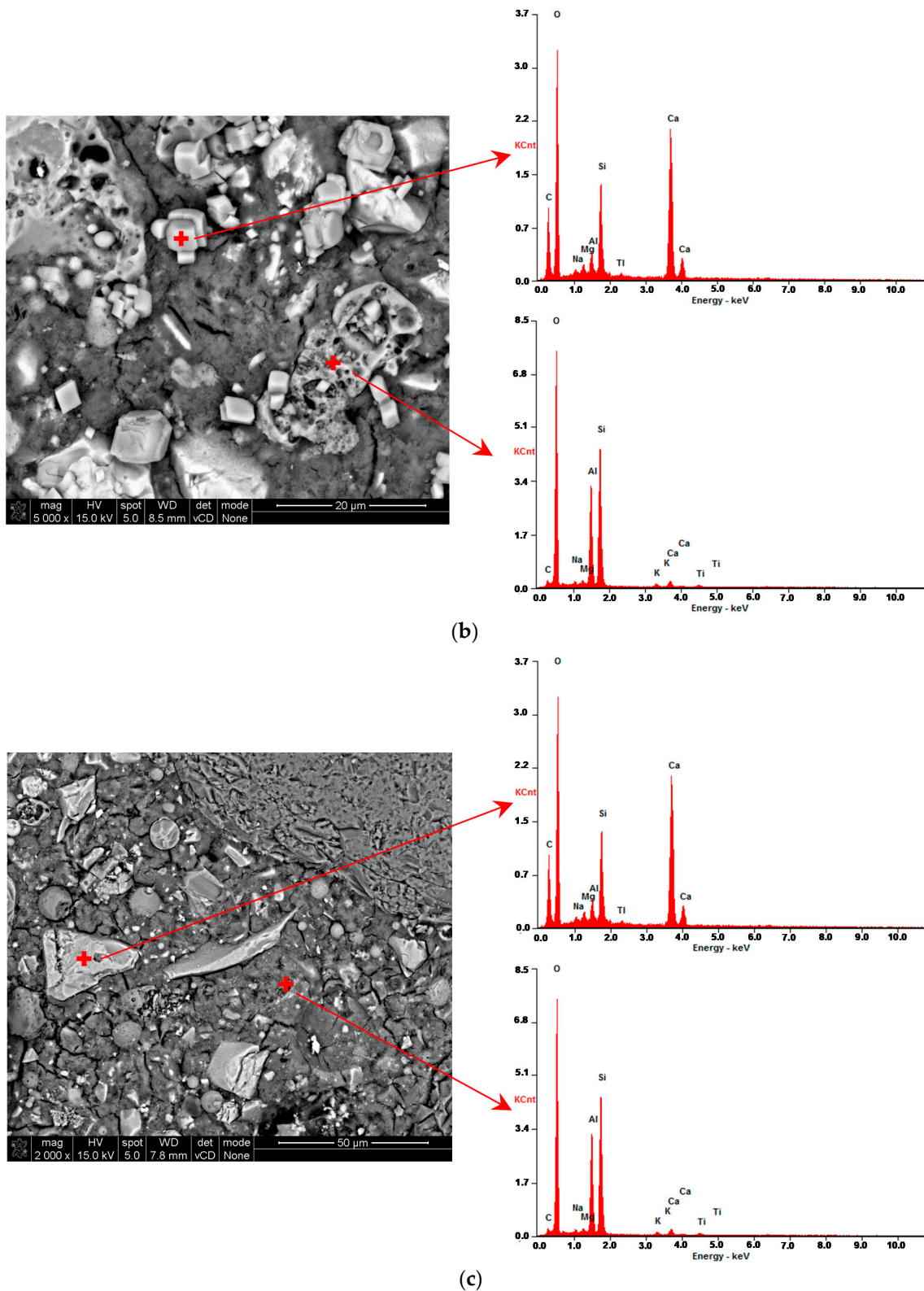


Figure 8. EDS analysis results at indicated points of (a) C55_SFA15_SF3, (b) C100_SFA15_SF3, and (c) C100_SFA30_SF3 samples.

3.7. pH Value

The pH values of 1:1 solutions of fine crushed concrete in distilled water were equal to 12.1 for the mixtures C100_SFA15_SF3, C100_SFA30_SF3, and 12.0 for the mixture C55_SFA15_SF3. Therefore, it can be stated that the alkalinity of the concrete decreases

with increasing GGBFS amount. An increase in the FA content to 30% in C100_SFA30_SF3 did not reduce the pH value of HPC. The tested pH values did not limit the use of designed HPC in aggressive carbonation environments considering the ability to protect the passive film on the surface of steel reinforcement bars.

4. Conclusions

Based on the research conducted, the following conclusions were drawn:

- It is possible to obtain High-Performance Concrete while greatly reducing the amount of Portland cement clinker in the concrete mix (64–114 kg/m³). The designed HPCs reached compressive strength of 76.1–91.7 MPa after 28 days of curing and 88.0–99.9 MPa after 90 days of curing.
- Low-clinker eco-efficient HPCs were characterized by a very slow to slow rate of compressive strength development within the first 28 days of curing according to EN 206 f_{cm2}/f_{cm28} ratio. However, the differences between 2-day and 28-day compressive strength values were the highest (from 420% to 957%) compared with the further curing periods: 28-day–90-day (9–16%) and 90-day–730-day (0.8–1.4%).
- Commonly used compressive strength development models insufficiently described the properties of low-clinker HPC, greatly overestimating the early age compressive strength. However, the differences between the estimated and tested values decreases in the long curing period.
- None of the recommended elastic modulus development models made it possible to estimate HPC modulus of elasticity after long curing period with acceptable precision. Basic variants of the proposed models underestimated the elastic modulus, while the corrected Eurocode 2 model overestimated the value of modulus of elasticity.
- All the designed HPCs, due to incorporating high GGBFS content, SCMs and maintaining low water/binder ratio, were frost resistant after 56 days of curing without the addition of air-entraining admixtures.
- The high density and homogeneity of the HPC binder matrix have been confirmed by means of SEM microstructure analysis and tests of depth of water penetration under pressure.
- The microstructure of the HPC was dependent on the binder composition. Replacement of the 45% of cement by the GGBFS resulted in a significantly higher amount of unreacted slag grains in the microstructure. The higher content of SCMs in the binder was associated with the smaller amount of calcite crystals as an effect of carbonation at the same depth. A lot of microcracks were observed for the binder matrix with higher amounts of Portland cement clinker. Still, it was impossible to determine with certainty whether there was a relation between the amount of Portland cement clinker and the number of microcracks.
- pH value tests confirmed that the low-clinker HPCs retained their protective properties in relation to steel reinforcement.

Author Contributions: Conceptualization, W.J.-R. and K.K.; methodology, K.K., W.J.-R. and K.C.; software, K.K. and K.C.; validation, W.J.-R. and K.C.; formal analysis, W.J.-R.; investigation, K.K., W.J.-R. and K.C.; resources, W.J.-R.; data curation, K.K. and K.C.; writing—original draft preparation, K.K.; writing—review and editing, K.C. and W.J.-R.; visualization, K.K. and K.C.; supervision, W.J.-R.; project administration, W.J.-R.; funding acquisition, W.J.-R. All authors have read and agreed to the published version of the manuscript.

Funding: This research received no external funding. The APC was funded by the Strategic Research Project of the Warsaw University of Technology: “Circular Economy”.

Institutional Review Board Statement: Not applicable.

Informed Consent Statement: Not applicable.

Data Availability Statement: Not applicable.

Acknowledgments: The authors would like to thank Górażdże Cement S.A. for providing CEM III/B and GGBFS samples and Warbud-Beton Sp. z o.o. for providing SFA and SF samples as well as for the technical support.

Conflicts of Interest: The authors declare no conflict of interest. The funders had no role in the design of the study; in the collection, analyses, or interpretation of data; in the writing of the manuscript, or in the decision to publish the results.

References

1. Olivier, J.G.J.; Peters, J.A.H.W. *Trends in Global CO₂ and Total Greenhouse Gas Emissions: 2019 Report*; PBL Netherlands Environmental Assessment Agency: The Hague, The Netherlands, 2020; p. 12.
2. Bernhardt, D.; Reilly, J.F., II. *Mineral Commodity Summaries 2020*; U.S. Geological Survey: Reston, VA, USA, 2020; p. 43. [[CrossRef](#)]
3. Müller, N.; Harnisch, J. *A Blueprint for a Climate Friendly Cement Industry*; WWF—Lafarge Conservation Partnership Report; WWF International: Gland, Switzerland, 2008; p. 7.
4. Leese, R.; Casey, D. *Fact Sheet 18. Embodied CO₂e of UK Cement, Additions and Cementitious Material*; MPA Cement: London, UK, 2019.
5. Matthes, W.; Vollpracht, A.; Villagrán, Y.; Kamali-Bernard, S.; Hooton, D.; Gruyaert, E.; Soutsos, M.; De Belie, N. Ground Granulated Blast-Furnace Slag. In *Properties of Fresh and Hardened Concrete Containing Supplementary Cementitious Materials. State-of-the-Art Report of the RILEM Technical Committee 238-SCM, Working Group 4*; De Belie, N., Soutsos, M., Gruyaert, E., Eds.; Springer: Cham, Switzerland, 2018; Volume 25, pp. 13–17. [[CrossRef](#)]
6. Benhelal, E.; Zahedi, G.; Shamsaei, E.; Bahadori, A. Global strategies and potentials to curb CO₂ emissions in cement industry. *J. Clean. Prod.* **2013**, *51*, 142–161. [[CrossRef](#)]
7. Samad, S.; Shah, A. Role of binary cement including Supplementary Cementitious Material (SCM), in production of environmentally sustainable concrete: A critical review. *Int. J. Sustain. Built Environ.* **2017**, *6*, 663–674. [[CrossRef](#)]
8. Aitcin, P.C. The durability characteristics of high performance concrete: A review. *Cem. Concr. Compos.* **2003**, *25*, 409–420. [[CrossRef](#)]
9. Pal, S.C.; Mukherjee, A.; Pathak, S.R. Investigation of hydraulic activity of ground granulated blast furnace slag in concrete. *Cem. Concr. Res.* **2003**, *33*, 1481–1486. [[CrossRef](#)]
10. Bouikni, A.; Swamy, R.N.; Bali, A. Durability properties of concrete containing 50% and 65% slag. *Constr. Build. Mater.* **2009**, *23*, 2836–2845. [[CrossRef](#)]
11. Sabet, D.B.; Lim, T.Y.D.; Teng, S. Durability Properties and Microstructure of Ground Granulated Blast Furnace Slag Cement Concrete. *Int. J. Concr. Struct. Mater.* **2014**, *8*, 157–164. [[CrossRef](#)]
12. Teng, S.; Lim, T.Y.D.; Sabet, B.D. Durability and mechanical properties of high strength concrete incorporating ultra fine Ground Granulated Blast-furnace Slag. *Constr. Build. Mater.* **2013**, *40*, 875–881. [[CrossRef](#)]
13. Bagheri, A.R.; Zanganeh, H.; Moalemi, M.M. Mechanical and durability properties of ternary concretes containing silica fume and low reactivity blast furnace slag. *Cem. Concr. Compos.* **2012**, *34*, 663–670. [[CrossRef](#)]
14. Ganesh, P.; Ramachandra Murthy, A. Tensile behaviour and durability aspects of sustainable ultra-high performance concrete incorporated with GGBS as cementitious material. *Constr. Build. Mater.* **2019**, *197*, 667–680. [[CrossRef](#)]
15. Shi, H.; Xu, B.; Zhou, X. Influence of mineral admixtures on compressive strength, gas permeability and carbonation of high performance concrete. *Constr. Build. Mater.* **2009**, *23*, 1980–1985. [[CrossRef](#)]
16. Zhang, X.; Gao, K.; Zhou, X.; Wang, H. Studies on influence of mineral admixtures on high performance concrete gas permeability. *Appl. Mech. Mater.* **2011**, *99–100*, 762–767. [[CrossRef](#)]
17. Askarnejad, S.; Rahbar, N. Effects of cement–polymer interface properties on mechanical response of fiber-reinforced cement composites. *J. Nanomech. Micromech.* **2017**, *7*, 04017002. [[CrossRef](#)]
18. Giergiczny, Z.; Król, A.; Talaj, M.; Wandoch, K. Performance of Concrete with Low CO₂ Emission. *Energies* **2020**, *14*, 4238. [[CrossRef](#)]
19. Atis, C.D.; Bilim, C. Wet and dry cured compressive strength of concrete containing ground granulated blast-furnace slag. *Build. Environ.* **2007**, *42*, 3060–3065. [[CrossRef](#)]
20. Lämmlein, T.D.; Messina, F.; Wyrzykowski, M.; Terrasi, G.P.; Lura, P. Low clinker high performance concretes and their potential in CFRP-prestressed structural elements. *Cem. Concr. Compos.* **2019**, *100*, 130–138. [[CrossRef](#)]
21. Dave, N.; Misra, A.K.; Srivastava, A.; Sharma, A.K.; Kaushik, S.K. Study on quaternary concrete micro-structure, strength, durability considering the influence of multi-factors. *Constr. Build. Mater.* **2017**, *139*, 447–457. [[CrossRef](#)]
22. Lewis, R.C. Silica fume. In *Properties of Fresh and Hardened Concrete Containing Supplementary Cementitious Materials. State-of-the-Art Report of the RILEM Technical Committee 238-SCM, Working Group 4*; De Belie, N., Soutsos, M., Gruyaert, E., Eds.; Springer: Cham, Switzerland, 2018; Volume 25, pp. 106–107. [[CrossRef](#)]
23. Riedel, P.; Leutbecher, T. Effect of specimen size on the compressive strength of ultra-high performance concrete. In Proceedings of the AFGC-ACI-fib-RILEM Int. Symposium on Ultra-High Performance Fibre-Reinforced Concrete, UHPFRC 2017, Montpellier, France, 2–4 October 2017; pp. 251–260.

24. ACI Committee 209, The United States. ACI 209R-92, Prediction of Creep, Shrinkage, and Temperature Effects in Concrete Structures. 1992. Reapproved 1997. Available online: https://worldarchi.com/wp-content/uploads/2019/05/209r_92.pdf (accessed on 20 October 2020).
25. Japan Society of Civil Engineers. *JSCE Guidelines for Concrete No. 15: Standard Specifications for Concrete Structures—2007 “Design”*; Japan Society of Civil Engineers (JSCE): Tokyo, Japan, 2011.
26. European Committee for Standardization. *EN 1992-1-1, Eurocode 2—Design of Concrete Structures—Part 1-1: General Rules and Rules for Buildings*; CEN: Brussels, Belgium, 2004.
27. International Federation for Structural Concrete (FIB). *CEB-FIP Model Code for Concrete Structures 2010*; Wilhelm Ernst & Sohn: Berlin, Germany, 2013.
28. Klemczak, B.; Batog, M.; Pilch, M. Assessment of concrete strength development models with regard to concretes with low clinker cements. *Arch. Civ. Mech. Eng.* **2016**, *16*, 235–247. [[CrossRef](#)]
29. Mierzwa, J. Concrete strength development function according to MC 2010 in the light of tests. *Procedia Eng.* **2015**, *108*, 655–663. [[CrossRef](#)]
30. ACI Committee 363. State-of-art-report on high strength concrete. *ACI Mater. J.* **1984**, *81*, 364–411.
31. Norwegian Council for Building Standardization. *Concrete Structures Design Rules NS 3473*; Norwegian Concrete Association: Stockholm, Sweden, 1992.
32. Chao-Qun, L.; Ravindra, K.D.; Gurmel, S.G. Carbonation resistance of GGBS concrete. *Mag. Concr. Res.* **2016**, *68*, 936–969.
33. Bisschop, J.; van Mier, J.G.M. Shrinkage Microcracking in Cement-based Materials with Low Watercement Ratio. In Proceedings of the RILEM International Conference on Early Age Cracking in Cementitious Systems (EAC’01), Haifa, Israel, 12–14 March 2001; Volume 1.